Published in final edited form as:
J Clin Oncol. 2015 November 20; 33(33): 3911–3920. doi:10.1200/JCO.2014.59.1503.

Mutational Spectrum, Copy Number Changes, and Outcome: Results of a Sequencing Study of Patients With Newly Diagnosed Myeloma

Brian A Walker[#1], **Eileen M Boyle**[#1], **Christopher P Wardell**[1], **Alex Murison**[1], **Dil B Begum**[1], **Nasrin B Dahir**[1], **Paula Z Proszek**[1], **David C Johnson**[1], **Martin F Kaiser**[1], **Lorenzo Melchor**[1], **Lauren I. Aronson**[1], **Charlotte Pawlyn**[1], **F Mirabella**[1], **John R. Jones**[1], **Annamaria Brioli**[1], **Aneta Mikulasova**[2], **Xavier Leleu**[3], **David A Cairns**[4], **Walter Gregory**[4], **A Quartilho**[4], **Mark T Drayson**[5], **Nigel Russell**[6], **Gordon Cook**[7], **Graham H Jackson**[8], **Faith E Davies**[1], and **Gareth J Morgan**[1]

[1]Division of Molecular Pathology, The Institute of Cancer Research, London, United Kingdom

[2]Department of Experimental Biology, Faculty of Science, Masaryk University, CZ

[3]Department of Haematology, Lille University Hospital, Lille, France

[4]Clinical Trials Research Unit, Leeds Institute of Clinical Trial Research, University of Leeds, Leeds, United Kingdom

[5]Clinical Immunology, School of Immunity & Infection, University of Birmingham, Birmingham, United Kingdom

[6]Centre for Clinical Haematology, Nottingham University Hospital, Nottingham, United Kingdom

[7]Section of Experimental Haematology, Leeds Institute of Cancer & Pathology, University of Leeds, Leeds, United Kingdom

[8]Department of Haematology, Newcastle University, Newcastle-Upon-Tyne, United Kingdom

[#] These authors contributed equally to this work.

Abstract

Purpose—At the molecular level myeloma is characterised by copy number abnormalities and recurrent translocations into the immunoglobulin heavy chain (*IGH*) locus. Novel methodologies such as massively parallel sequencing have begun to describe the pattern of tumour acquired mutations but their clinical relevance has yet to be established.

Methods—We have performed whole exome sequencing on 463 presenting myeloma patients enrolled in the NCRI Myeloma XI trial (NCT01554852) for which complete molecular cytogenetic and clinical outcome data are available.

Results—We identified 15 significantly mutated genes comprising *IRF4*, *KRAS*, *NRAS*, *MAX*, *HIST1H1E*, *RB1*, *EGR1*, *TP53*, *TRAF3*, *FAM46C*, *DIS3*, *BRAF*, *LTB*, *CYLD* and *FGFR3*. The

Corresponding author: Professor Gareth Morgan, Division of Molecular Pathology, The Institute of Cancer Research, London, SM2 5NG. gareth.morgan@icr.ac.uk. Telephone: +44 2087224130, Fax: +44 2087224432.

Europe PMC Funders Author Manuscripts

mutational spectrum is dominated by mutations in the RAS (43%) and NF-κB (17%) pathway, but while they are prognostically neutral they could be targeted therapeutically. Mutations in *CCND1* and DNA repair pathway alterations (*TP53*, *ATM*, *ATR* and *ZNFHX4* mutations) are associated with a negative impact on survival. In contrast, those in *IRF4* and *EGR1* are associated with a favourable overall survival. We have combined these novel mutation risk factors with the recurrent molecular adverse features and ISS to generate an ISS–MUT score that can identify a high-risk population that relapse and die prematurely.

Conclusion—We have refined our understanding of genetic events in myeloma and identified clinically relevant mutations that may be used to better stratify patients at presentation.

Introduction

Myeloma arises following the immortalisation of a plasma cell that subsequently acquires further genetic abnormalities leading to an increasingly malignant phenotype[1]. While the treatment of myeloma has improved with increasing numbers of survivors beyond ten years from diagnosis there are still a significant number of patients with both short progression-free survival (PFS) and overall survival (OS)[2-4]. It is important to identify these "high-risk" patients and to design trials aimed at improving their outcome. Traditionally, prognosis has been assessed by the use of clinical data such as the international staging system (ISS)[3,5], but for individual patients this is insufficient to direct treatment. ISS can be improved by the addition of molecular cytogenetic data[2,3] but this does not describe the full extent of the risk and could be improved by more comprehensively describing the genetic features of the disease and using it to define outcome.

The main clinically relevant molecular sub-groups of myeloma are defined by the balanced translocations into the *IGH* locus at 14q32[6-8] and copy number abnormalities (CNA). The translocation subgroups include the t(4;14) (13%) and the t(14;16)/t(14;20) translocated subgroups (5%) which are associated with poor prognosis with respective overall survival ranging from 22-60 months and 16-30 months, and the t(11;14) (13%) which is associated with a favourable prognosis (OS >5-10 years) [2,8-10].(More recently both the prevalence and adverse prognostic significance associated with *MYC* translocations (20%) has been realised (median OS 24 months) [11]. A further set of clinically important prognostic abnormalities are defined by recurrent CNA the full spectrum of which have been defined by genome mapping experiments[12]. The clinically important copy number abnormalities include hyperdiploidy (HRD), associated with favourable prognosis, and gain(1q) (38%), del(1p) (8.4%), del(17p) (9.5%) and del(12p) (8.9%) being associated with adverse prognosis [2,9].

We have used FISH previously to show that patients with a greater number of adverse cytogenetic abnormalities have impaired clinical outcomes[2]. It has become clear that the value of these tests could be improved by identifying all of the prognostically important genetic abnormalities present and using all of the information to risk-stratify patients. A key technology with which to identify these abnormalities is whole exome sequencing plus a targeted pull down of regions of interest, which can identify structural variants as well as the spectrum of mutations[13-15]. In this study we have used such an approach on 463 presenting samples entered into a clinical trial and have used the data generated to define both the

Europe PMC Funders Author Manuscripts

pattern of mutations and how they relate to survival. We have then combined this with the ISS to generate a predictive score to define high-risk clinical behaviour, which we term ISS-MUT.

Methods

Patient Samples

Samples were taken, following informed consent, from patients newly diagnosed with symptomatic myeloma and enrolled in the NCRI Myeloma XI trial (NCT01554852, CRUK/09/014). This is a phase III, open-label trial where patients were randomised between triplet immunomodulatory drug (IMiD) induction of either cyclophosphamide, thalidomide, dexamethasone (CTD) or cyclophosphamide, lenalidomide, dexamethasone (CRD). Patients with a suboptimal response (<very good partial response) were randomised to pre-transplant treatment with a proteasome inhibitor triplet (cyclophosphamide, bortezomib, dexamethasone, CVD). Older or less fit patients had appropriate dose reductions and did not receive an autologous stem cell transplant. All patients subsequently underwent further randomisation to either no maintenance, lenalidomide maintenance or lenalidomide and vorinostat maintenance, Overview of the Myeloma XI trial diagram. PFS and OS were measured from initial randomisation and the median (range) follow-up was 25 months (0.09, 42.97). The patient demographics are presented in Supplementary Table 1. The median PFS was 26.6 months (95%CI (23.6, 29.9)) and the 3-year overall survival rate was 66% (95%CI (60, 73)).

Exome Sequencing and mutation calling

Plasma cells were isolated from bone marrow samples using CD138+ MACSorting (Miltenyi Biotech, Bisley, UK). DNA from both tumour and peripheral blood were used in the exome capture protocol as previously described[16]. FastQC (v0.10.0) was used for basic quality control of Illumina paired-end sequencing data. Single nucleotide variants (SNVs) were called using MuTect (v1.1.4). Copy number across the exome was determined using Control-FREEC and Cancer Clonal fraction (CCF) calculated[17].

Molecular cytogenetics

Translocations were called[18] and manually curated. Simultaneously, translocations were determined by qRT-PCR[19]. When not concordant, the data were examined and a decision made. Copy number changes were assessed by Multiplex Ligation-Dependent Amplification using the SALSA P425-B1 probe mix (MRC-Holland, Amsterdam, The Netherlands)[20]. Copy number at each locus was estimated[21] and determined as previously described[22].

Correlation studies

Correlation between mutated genes and cytogenetic abnormalities using Bayesian inference was determined using the program "JAGS"[23] and the R-interface Bayesmed [2425]. The probability of the observed data under the null hypothesis versus the alternative hypothesis or Bayes factor (BF) was computed. BF>1 was considered significant. BF 1-3, 3-20, 20-150 and >150 were considered weak, positive, strong and very strong associations respectively[26]. Correlation coefficients were plotted using corrplot[27].

Survival analysis

Time-to-event analysis was performed in R[28] using the survival[29,30] and coin[31,32] packages. Differences between survival functions were tested using the logrank test. Hazard ratios were estimated from Cox proportional hazard regression. All statistical tests were two-sided and evaluated at the 5% level. Power to detect prognostic associations was estimated using PowerSurvEpi[33]. Multivariable stepwise variable selection was performed using a standard backward elimination approach with $p<0.05$ taken as level of significance for variable retention to estimate an apparent predictive ability quantified using Harrell's C-index. This predictive ability was then internally validated with a bootstrap resampling strategy using the package rms[34] and the validate function where the stepwise selection strategy was also repeated. This analysis used 400 resamples and estimated an optimism-corrected C-index. Further details may be found in the Supplementary Methods.

Results

Significantly mutated genes and altered pathways

We identified 13 significantly mutated genes, Table 1, including *KRAS*, *NRAS*, *TRAF3*, *TP53*, *FAM46C*, *DIS3*, *BRAF*, *LTB*, *CYLD*, *RB1*, *HIST1H1E*, *IRF4* and *MAX*. The location of the mutations may be found in Supplementary Figure 1.

The RAS/MAPK pathway is the most frequently mutated pathway (*KRAS*=21.2%, *NRAS*=19.4%, *BRAF*=6.7%) making up a total of 43.2% of patients with *NRAS* and *KRAS* tending to be mutually exclusive, but co-occurring in 2% of patients. They had no impact on survival, Supplementary Figure 2. The mean CCF for *KRAS*, *NRAS* and *BRAF* were 32%, 33% and 25% suggesting they are associated with progression. The hotspots of mutation in *KRAS* and *NRAS* included codons 12, 13 and 61 as well as codon 600 in BRAF, Supplementary Table 2-3.

Mutational activation of the NF-κB pathway genes[35], Supplementary Figure 3, important in late B-cell development was seen. A total of 27 mutated genes falling within these pathways were identified, accounting for 17% of cases. These genes included *TRAF3* (mutated in 3.7% and deleted in 13%), *CYLD* (mutated in 2.4% and deleted in 17%) and *LTB* (mutated in 3% of cases). The key plasma-cell survival gene and target of the IMiD drugs, *IRF4*, is mutated in 3.2% of cases, including eight cases with p.K123R. The pattern of these mutations and the down-regulation of *MYC* expression in these patients suggest they are activating. We identified mutations in another IMiD target gene[36], *EGR1* (n=17), all of which are located at the 5' end of the gene.

We identified *TP53* variants in 11% of cases (del(17p) in 9.5% and *TP53* mutations in 3% of cases). Other mutated genes associated with the delivery of an apoptotic signal included *ATM* and *ATR*. Loss of *ATM* was seen in 1.3% and was mutated in 3% with *ATR* mutations and deletions seen in 1.5% of samples, resulting in combined *TP53*, *ATM and ATR* abnormalities present in 14.5% of patients. These abnormalities were seen in other datasets with similar frequencies (Supplementary Table 4, Supplementary Figures 4-5).

Association of Mutated Genes with Cytogenetic Sub-groups

Significantly mutated genes were seen within the cytogenetic sub-groups, Table 1. *FGFR3*, located on the der(14), is only mutated in the t(4;14) group where activating mutations are found in 17% of cases. *CCND1* is significantly mutated in the t(11;14) subgroup (12% of cases) whereas the transcriptional regulator *EGR1*, is significantly mutated in the hyperdiploid samples. Integrating our data with previously published data[13,15] established a series of 733 cases and identified 5 additional significantly mutated genes including *PRDM1*, *BCL7A*, *ATRIP*, *NRM* and *PRKD2*, Supplementary Table 5. *PRKD2* mutations, which were present in 2.3% of cases, were correlated to t(4;14).

A number of adverse prognostic lesions were seen to co-segregate including t(4;14), del(13q), and gain(1q), Figure 1 and Supplementary Table 6. The t(11;14) was associated with *KRAS* and *IRF4* mutations. Del(12p) was associated with t(4;14) and del(17p). *MYC* translocations were weakly correlated to HRD.

Within the region of del(12p) mutations in *CHD4* were identified in 9 patients and deletions in 9% of patients. CHD4 interacts with ZFHX4 to modulate p53 function and mutations in *ZFHX4* were seen in 20 cases, Supplementary Figure 6-Figure 3A.

Survival analysis—We carried out a time-to-event analysis of PFS and OS using the markers outlined above which included mutations occurring more than 10-times (excluding structural and housekeeping genes), copy number and structural abnormalities (CNSA) and mutated pathways with clinical features. This analysis had 80% power to identify features with a hazard ratio (HR) greater than 2.31 for PFS and 2.94 for OS, Supplementary Table 7. The dataset as a whole behaved as expected with negative associations being found for higher ISS stages, creatinine >150 μM, amp(1q), del(17p), *MYC* translocations, t(4;14), del(13q), del(1p32) and del(12p) and positive associations for hyperdiploidy, Table 2. Amp(1q) was prognostically relevant and seemed to drive the prognostic impact of gain(1q) (PFS: HR 1.8; 95%CI (1.2, 2.76); p=0.004 and OS HR 2.7; 95%CI (1.6, 4.5); p=0.0002), Figure 2A-B. Del(1p32) variants (including deletions and mutations) had a negative impact on OS (2y-OS 62%; 95%CI (48,79) versus 81%; 95%CI (77, 85); p=0.001), but not PFS (median 22.8 months; 95%CI (17.6, ∞) versus 26.7; 95%CI (24.0, 29.9); p=0.33).

For the first time we are able to examine the impact of mutations discovered in a non-biased fashion on survival within a large clinical trial. We found that *CCND1* mutations were associated with a negative impact on OS (2y-OS 38.1%; 95%CI (14, 100) versus 80% 95%CI (76, 84); p=0.005) (Supplementary Figure 7).

Inability to deliver an apoptotic signal was an important prognostic marker. Del(17p) and *TP53* mutations have a significant negative impact on outcome (Figure 2C-D and Supplementary Figure 4). *ATM* mutations were associated with a trend towards impaired PFS (median 15.4 months; 95%CI (8.67, ∞) versus 26.6 months 95%CI (24.0, 30.0); p=0.05) and impaired OS (2y-OS 50%; 95%CI (30, 84) versus 80.3%; 95%CI (76, 84); p=0.01). *ATR* mutations were seen in 1.5% of cases and have a similar impact on prognosis in terms of PFS (median 23.9 months; 95%CI (10.35, ∞) versus 26.6 months; 95%CI (24.0, 29.9); p=0.3) and OS (2y-OS 67%; 95%CI (38, 100) versus 80%; 95%CI (76, 84); p=0.05).

Combined together, *ATM* and *ATR* mutations, and *TP53* mutations and del(17p) had a significant impact on both PFS and OS, Figure 2E-F and Supplementary Table 8. Mutations in *ZFHX4*, are associated with a negative impact on PFS (median 8.8 months; 95%CI (8.05, ∞) versus 26.9 months; 95%CI (25.0, 30.2); p<0.001), but not OS (2y-OS 72%; 95%CI (54, 96) versus 80%; 95%CI (76, 84); p=0.5). *NCKAP5*, coding for a Nck-adaptor protein, was associated with an adverse OS, Table 2 and Supplementary Figure 7-8.

Mutations in *IRF4* had a positive impact on survival with a trend towards an improvement in PFS (2y-PFS 71%; 95%CI (50, 100) versus 54%; 95%CI (49, 60); p=0.09) and a significant impact on OS (2y-OS 100% versus 79%; 95%CI (75, 83); p=0.05), Figure 3B. Mutations in *EGR1* had a positive impact on survival with a trend towards an improvement on PFS (median 35.1 months; 95% CI (26.1, ∞) versus 26.2 months; 95%CI (23.7, 28.7); p=0.14) and a significant impact on OS (2y-OS 100% versus 78%; 95%CI (75, 83); p=0.04), Figure 3C.

In a multivariable analysis for PFS, ISSIII, age>70, t(4;14), *MYC* translocations, *TP53* variants, *ATM/ATR* mutations, *ZFHX4* mutations, remained independent prognostic factors, Figure 4A. The apparent C-index was 0.67 with the bootstrap resampling strategy suggesting an optimism of 0.02, i.e. an internally validated C-index penalized for potential over-fitting of 0.65.

In a multivariable analysis for OS, ISS III, *TP53* variants, *CCND1* mutations, *ATM/ATR* mutations, amp(1q) and *MYC* translocations, remained independent, Figure 4A. The apparent C-index was 0.65 with the bootstrap resampling strategy suggesting an optimism of 0.06, i.e. an internally validated C-index of 0.59.

Cumulative negative impact of mutations

We have previously shown that integrating ISS with CNSA is a key determinant of prognosis[2]. We further extended this to include poor prognosis mutations (MUT) including *TP53*, *ZFHX4*, *CCND1* and *ATM/ATR* and novel CNSA such as *MYC* translocations and amp(1q). Using a CNSA-MUT score we were able to identify 4 different prognostic populations representing 50%, 33%, 11%, 2% of the population studied with increasingly poor PFS (one lesion: HR=1.7, p=0.0007; 2 lesions: HR=3.4, p<0.0001 and 3 lesions: HR=15.2, p<0.0001) and OS (one lesion: HR=2.0, p=0.002, 2 lesions: HR=4.8 p<0.0001, 3 lesions: HR=9.6, p<0.0001). A high-risk population can be identified comprising cases with 2 or more adverse features representing 13% of patients that both relapsed (median PFS 10.6 months; 95%CI (8.7, 17.9) versus 28.5 months; 95%CI (26.3, 31.3); p<0.0001) and died prematurely (2y-OS 45%; 95%CI (7, 33) versus 83%; (82, 89); p<0.0001). Nevertheless, using this acquired genetic lesion approach we show that 35% of patients that relapse before 18 months and 27% of patients that died before 24 months were not detected, Supplementary Figure 9.

In order to address this issue we incorporated the clinical information captured by the ISS, as has been done previously[3]. In this analysis combining CNSA and mutations with ISS, ISS-MUT, we identified 3 prognostic groups (Group 1: ISS I/II with no CNSA or mutation, Group 2: ISS III with no CNSA or mutation or ISS I/II/III with one CNSA or mutation,

Group 3: Two CNSA or mutation regardless of their ISS). This approach adds sensitivity to the detection of early progression (EP) and early mortality (EM) (80.5% versus 65% for EP and 90% versus 75% for EM) (Supplementary Figure 9-10).

Discussion

We have identified the recurrent mutations characterising presentation myeloma and their impact on survival within this treatment setting. We show that there are a limited number of recurrent variants that are seen in a significant proportion of cases and that they co-segregate with the known recurrent CNSA typical of myeloma. Minimal differences in significantly mutated genes were seen between the major etiologic subtypes of myeloma and it seems likely that, once initiated, it is the same mutated pathways which push the disease forward. Based on this analysis and previous work, myeloma is clearly a disease driven by RAS pathway mutations and by *MYC* translocations[11].

With the exception of *NRAS* and *KRAS*, all genes are mutated at a low percentage indicating the deregulation of key pathways, rather than mutations of single genes, could be important. We identified the central role of deregulation of the RAS/MAPK, the NF-κB pathway and apoptotic response, but interestingly mutation of the RAS/MAPK or NF-κB had no prognostic relevance in this clinical trial.

However, the inability to deliver an effective apoptotic response to DNA damage gave the most significantly prognostic mutational marker in this trial. Combining the known poor prognostic marker *TP53*[2,3,37] with additional mutations in *ATM* or *ATR* identifies 17% of presenting cases that have a significantly poor outcome. Mutations in *ATM* are known poor prognostic markers in CLL[38,39], mantle cell[40] and acute lymphoblastic T cell leukaemia[41], but their prognostic impact has, until now, not been examined in myeloma[42]. *ATR* mutations, especially truncating mutations in exon 10, have been associated with a loss of function and an adverse prognosis in endometrial cancer[43]. Beyond *ATM* and *ATR*, we identified mutations in other members of the DNA-Damage-Repair (DDR) pathway including *ZFHX4*, member of the NuRD complex, involved in chromatin refolding [44,45,46]. These data would suggest that patients with DNA repair pathway alterations may not benefit from alkylating agents, supporting the idea of therapy based on novel agents for these patients.

Myeloma XI is a trial based around IMiD drugs in which we have identified genes that are mutated and seem to have a positive impact on survival. In particular, we have identified mutations in *IRF4* and *EGR1*. IRF4 is believed to be downstream of the IMiD target cereblon and other proteins downstream namely IKZF1 and KPNA2, that have been linked to survival differences in IMiD treated patients[47]. However, mutations in these genes are infrequent compared to *IRF4*.

In myeloma, *EGR1* has recently been shown to be involved in recruitment of *MYC* to the promoters of *NOXA* and *BIM* inducing p53-independent apoptosis[48,49]. This is increased through bortezomib treatment where bortezomib enhances *MYC* and *EGR1* expression[49]. Furthermore, *EGR1* as a candidate gene for del(5q) in myelodysplastic syndromes has been

associated with response to lenalidomide[50]. The role of mutations at the 5' end of *EGR1* remains to be ascertained.

The detection of mutations can improve our ability to detect high-risk patients that relapse and die early, but who may benefit from specific therapeutic interventions. We have previously shown that integration of ISS and cytogenetic data (ISS-FISH) can identify high-risk and ultra-high-risk patients[2]. The further integration of mutational prognostic data can improve this to a molecular level. We have shown that the greater the number of adverse CNSA (t(4;14), del(17p), *MYC* translocations and amp(1q)) present within an individual patient, the worse the outcome. Adding both ISS and mutations, in our ISS-MUT score, adds precision to early mortality and progression detection, Supplementary Figure 9. The number of molecular features required to identify this high-risk group is small (n=9) and could easily be incorporated into a molecular diagnostic test which could be readily translated into the modern molecular diagnostic laboratory. This predictive tool must be externally validated in further patient sample, but internal validation undertaken indicates robust predictive ability in bootstrap resamples.

The identification of actionable mutations within myeloma opens the way for targeted treatment. Key amongst these mutations in myeloma is the deregulation of the RAS/MAPK pathway with the most common being the recurrent mutations in *NRAS* and *KRAS* making it a major therapeutic target[44,51-53]. The other targetable pathway is NF-κB, which is consistently mutated in mature lymphoid malignancies, however, the spectrum of mutations seen in myeloma is different, Supplementary Figure 3D. Overall, we identified a set of potential actionable mutations comprising 309 targets applicable to 53% of patients. In the years to come we foresee this to increase to 440 targets applicable to 62% of patients, Table 3.

In summary, we have performed the first comprehensive molecular analysis of a clinical trial, in myeloma, that identifies key copy number and structural abnormalities and mutations that interact and identify high-risk patients who may benefit from alternative treatments.

Supplementary Material

Refer to Web version on PubMed Central for supplementary material.

Acknowledgements

The authors would like to thank all the patients and staff at centres throughout the UK whose participation made this study possible. The authors are grateful to the NCRI Haemato-oncology subgroup and to all principle investigators for their dedication and commitment to recruiting patients to the study. The principal investigators at the four top recruiting centres were Dr Don Milligan (Heart of England NHS Foundation Trust), Dr Jindriska Lindsay (Kent and Canterbury Hospital), Dr Nigel Russell (Nottingham University Hospital) and Dr Clare Chapman (Leicester Royal Infirmary). The support of the Clinical Trials Research Unit at The University of Leeds was essential to the successful running of the study and the authors would like to thank all the staff including Helen Howard, Corrine Collett, Jacqueline Ouzman and Alex Szubert. We also acknowledge The Institute of Cancer Research Tumour Profiling Unit for their support and technical expertise in this study.

Financial Support: This work was supported by a Myeloma UK program grant, Cancer Research UK CTAAC sample collection grants (C2470/A12136 and C2470/A17761) and a Cancer Research UK Biomarkers and Imaging Discovery and Development grant (C2470/A14261) as well as funds from the National Institute of Health

Biomedical Research Centre at the Royal Marsden Hospital. EMB was supported by the Fédération Française de Recherche sur le myélome et les gammapathies grant.

References

1. Morgan GJ, Walker BA, Davies FE. The genetic architecture of multiple myeloma. Nat Rev Cancer. 2012; 12:335–48. [PubMed: 22495321]
2. Boyd KD, Ross FM, Chiecchio L, et al. A novel prognostic model in myeloma based on co-segregating adverse FISH lesions and the ISS: analysis of patients treated in the MRC Myeloma IX trial. Leukemia. 2012; 26:349–55. [PubMed: 21836613]
3. Avet-Loiseau H, Durie BG, Cavo M, et al. Combining fluorescent in situ hybridization data with ISS staging improves risk assessment in myeloma: an International Myeloma Working Group collaborative project. Leukemia. 2013; 27:711–7. [PubMed: 23032723]
4. Klein U, Jauch A, Hielscher T, et al. Chromosomal aberrations +1q21 and del(17p13) predict survival in patients with recurrent multiple myeloma treated with lenalidomide and dexamethasone. Cancer. 2011; 117:2136–44. [PubMed: 21523726]
5. Greipp PR, San Miguel J, Durie BG, et al. International staging system for multiple myeloma. J Clin Oncol. 2005; 23:3412–20. [PubMed: 15809451]
6. Walker BA, Wardell CP, Johnson DC, et al. Characterization of IGH locus breakpoints in multiple myeloma indicates a subset of translocations appear to occur in pregerminal center B cells. Blood. 2013; 121:3413–9. [PubMed: 23435460]
7. Ross FM, Avet-Loiseau H, Ameye G, et al. Report from the European Myeloma Network on interphase FISH in multiple myeloma and related disorders. Haematologica. 2012; 97:1272–7. [PubMed: 22371180]
8. Avet-Loiseau H, Attal M, Moreau P, et al. Genetic abnormalities and survival in multiple myeloma: the experience of the Intergroupe Francophone du Myelome. Blood. 2007; 109:3489–95. [PubMed: 17209057]
9. Avet-Loiseau H, Li C, Magrangeas F, et al. Prognostic significance of copy-number alterations in multiple myeloma. J Clin Oncol. 2009; 27:4585–90. [PubMed: 19687334]
10. Fonseca R, Blood E, Rue M, et al. Clinical and biologic implications of recurrent genomic aberrations in myeloma. Blood. 2003; 101:4569–4575. [PubMed: 12576322]
11. Walker BA, Wardell CP, Brioli A, et al. Translocations at 8q24 juxtapose MYC with genes that harbor superenhancers resulting in overexpression and poor prognosis in myeloma patients. Blood Cancer J. 2014; 4:e191. [PubMed: 24632883]
12. Jenner MW, Leone PE, Walker BA, et al. Gene mapping and expression analysis of 16q loss of heterozygosity identifies WWOX and CYLD as being important in determining clinical outcome in multiple myeloma. Blood. 2007; 110:3291–300. [PubMed: 17609426]
13. Lohr JG, Stojanov P, Carter SL, et al. Widespread genetic heterogeneity in multiple myeloma: implications for targeted therapy. Cancer Cell. 2014; 25:91–101. [PubMed: 24434212]
14. Chapman MA, Lawrence MS, Keats JJ, et al. Initial genome sequencing and analysis of multiple myeloma. Nature. 2011; 471:467–72. [PubMed: 21430775]
15. Bolli N, Avet-Loiseau H, Wedge DC, et al. Heterogeneity of genomic evolution and mutational profiles in multiple myeloma. Nat Commun. 2014; 5:2997. [PubMed: 24429703]
16. Kozarewa I, Rosa-Rosa JM, Wardell CP, et al. A modified method for whole exome resequencing from minimal amounts of starting DNA. PLoS ONE. 2012; 7:e32617. [PubMed: 22403682]
17. Boeva V, Popova T, Bleakley K, et al. Control-FREEC: a tool for assessing copy number and allelic content using next-generation sequencing data. Bioinformatics. 2012; 28:423–5. [PubMed: 22155870]
18. Rausch T, Zichner T, Schlattl A, et al. DELLY: structural variant discovery by integrated paired-end and split-read analysis. Bioinformatics. 2012; 28:i333–i339. [PubMed: 22962449]
19. Kaiser MF, Walker BA, Hockley SL, et al. A TC classification-based predictor for multiple myeloma using multiplexed real-time quantitative PCR. Leukemia. 2013; 27:1754–7. [PubMed: 23318961]

Europe PMC Funders Author Manuscripts

20. Alpar D, de Jong D, Holczer-Nagy Z, et al. Multiplex ligation-dependent probe amplification and fluorescence in situ hybridization are complementary techniques to detect cytogenetic abnormalities in multiple myeloma. Genes Chromosomes Cancer. 2013; 52:785–93. [PubMed: 23720363]
21. Schwab CJ, Jones LR, Morrison H, et al. Evaluation of multiplex ligation-dependent probe amplification as a method for the detection of copy number abnormalities in B-cell precursor acute lymphoblastic leukemia. Genes Chromosomes Cancer. 2010; 49:1104–13. [PubMed: 20815030]
22. Boyle EM, Proszek P, Kaiser M, et al. A molecular diagnostic approach able to detect the recurrent genetic prognostic factors typical of presenting myeloma.
23. JAGS 3.4.0. Just Another Gibbs Sampler: (ed JAGS 3.4.0.). 2013.
24. Nuijten, M, Wetzels, R, Matzke, D, Dolan, CV, Wagenmakers, EJ. Default Bayesian hypothesis tests for correlation, partial correlation, and mediation, (ed 1.0). 2014.
25. Wetzels R, Wagenmakers EJ. A default Bayesian hypothesis test for correlations and partial correlations. Psychon Bull Rev. 2012; 19:1057–64. [PubMed: 22798023]
26. Kass R, Raferty A. Bayes Factors. Journal of the American Statistical Association. 1995; 90:773–795.
27. Wei, T. Corrplot: Visualization of a correlation matrix. 2013.
28. R development Core Team. R: A Language and Environment for Statistical Computing. R Foundation for Statistical Computing. R Foundation for statistical Computing; Vienna, Austria: 2013.
29. Therneau, T, Grambsch, P. Modeling Survival Data: Extending the Cox Model. Springer; New York: 2000.
30. Therneau, T. A Package for Survival Analysis in S, (ed R package version 2.37-7). 2014.
31. Hothorn T, Hornik K, van de Wiel M, et al. Implementing a Class of Permutation Tests: The {coin} Package. Journal of Statistical Software. 2008; 28:1–23. [PubMed: 27774042]
32. Hothorn T, Hornik K, van de Wiel M, et al. A Lego System for Conditional Inference. The American Statistician. 2006; 60:257–263.
33. Qiu, Weiliang; C, J, Lazarus, Ross; Rosner, Bernard; Jing, Ma. powerSurvEpi: Power and sample size calculation for survival analysis of epidemiological studies, (ed 0.0.6). 2012.
34. Harrell, FE. REGRESSION MODELING STRATEGIES with Applications to Linear Models, Logistic Regression, and Survival Analysis. Springer; 2001.
35. Annunziata CM, Davis RE, Demchenko Y, et al. Frequent engagement of the classical and alternative NF-kappaB pathways by diverse genetic abnormalities in multiple myeloma. Cancer Cell. 2007; 12:115–30. [PubMed: 17692804]
36. Chen L, Wang S, Zhou Y, et al. Identification of early growth response protein 1 (EGR-1) as a novel target for JUN-induced apoptosis in multiple myeloma. Blood. 2010; 115:61–70. [PubMed: 19837979]
37. Lode L, Eveillard M, Trichet V, et al. Mutations in TP53 are exclusively associated with del(17p) in multiple myeloma. Haematologica. 2010; 95:1973–6. [PubMed: 20634494]
38. Skowronska A, Austen B, Powell JE, et al. ATM germline heterozygosity does not play a role in chronic lymphocytic leukemia initiation but influences rapid disease progression through loss of the remaining ATM allele. Haematologica. 2012; 97:142–6. [PubMed: 21933854]
39. Guarini A, Marinelli M, Tavolaro S, et al. ATM gene alterations in chronic lymphocytic leukemia patients induce a distinct gene expression profile and predict disease progression. Haematologica. 2012; 97:47–55. [PubMed: 21993670]
40. Fang NY, Greiner TC, Weisenburger DD, et al. Oligonucleotide microarrays demonstrate the highest frequency of ATM mutations in the mantle cell subtype of lymphoma. Proc Natl Acad Sci U S A. 2003; 100:5372–7. [PubMed: 12697903]
41. Meier M, den Boer ML, Hall AG, et al. Relation between genetic variants of the ataxia telangiectasia-mutated (ATM) gene, drug resistance, clinical outcome and predisposition to childhood T-lineage acute lymphoblastic leukaemia. Leukemia. 2005; 19:1887–95. [PubMed: 16167060]

42. Austen B, Barone G, Reiman A, et al. Pathogenic ATM mutations occur rarely in a subset of multiple myeloma patients. Br J Haematol. 2008; 142:925–33. [PubMed: 18573109]
43. Zighelboim I, Schmidt AP, Gao F, et al. ATR mutation in endometrioid endometrial cancer is associated with poor clinical outcomes. J Clin Oncol. 2009; 27:3091–6. [PubMed: 19470935]
44. Matsuoka S, Ballif BA, Smogorzewska A, et al. ATM and ATR substrate analysis reveals extensive protein networks responsive to DNA damage. Science. 2007; 316:1160–6. [PubMed: 17525332]
45. Mu JJ, Wang Y, Luo H, et al. A proteomic analysis of ataxia telangiectasia-mutated (ATM)/ATM-Rad3-related (ATR) substrates identifies the ubiquitin-proteasome system as a regulator for DNA damage checkpoints. J Biol Chem. 2007; 282:17330–4. [PubMed: 17478428]
46. Chudnovsky Y, Kim D, Zheng S, et al. ZFHX4 interacts with the NuRD core member CHD4 and regulates the glioblastoma tumor-initiating cell state. Cell Rep. 2014; 6:313–24. [PubMed: 24440720]
47. Zhu YX, Braggio E, Shi CX, et al. Identification of cereblon-binding proteins and relationship with response and survival after IMiDs in multiple myeloma. Blood. 2014; 124:536–45. [PubMed: 24914135]
48. Boone DN, Qi Y, Li Z, et al. Egr1 mediates p53-independent c-Myc-induced apoptosis via a noncanonical ARF-dependent transcriptional mechanism. Proc Natl Acad Sci U S A. 2011; 108:632–7. [PubMed: 21187408]
49. Wirth M, Stojanovic N, Christian J, et al. MYC and EGR1 synergize to trigger tumor cell death by controlling NOXA and BIM transcription upon treatment with the proteasome inhibitor bortezomib. Nucleic Acids Res. 2014
50. Joslin JM, Fernald AA, Tennant TR, et al. Haploinsufficiency of EGR1, a candidate gene in the del(5q), leads to the development of myeloid disorders. Blood. 2007; 110:719–26. [PubMed: 17420284]
51. Mulligan G, Lichter DI, Di Bacco A, et al. Mutation of NRAS but not KRAS significantly reduces myeloma sensitivity to single-agent bortezomib therapy. Blood. 2014; 123:632–9. [PubMed: 24335104]
52. Takahashi N, Yamada Y, Taniguchi H, et al. Clinicopathological features and prognostic roles of KRAS, BRAF, PIK3CA and NRAS mutations in advanced gastric cancer. BMC Res Notes. 2014; 7:271. [PubMed: 24774510]
53. Bruce S, Leinonen R, Lindgren CM, et al. Global analysis of uniparental disomy using high density genotyping arrays. J.Med.Genet. 2005; 42:847–851. [PubMed: 15879501]

Europe PMC Funders Author Manuscripts

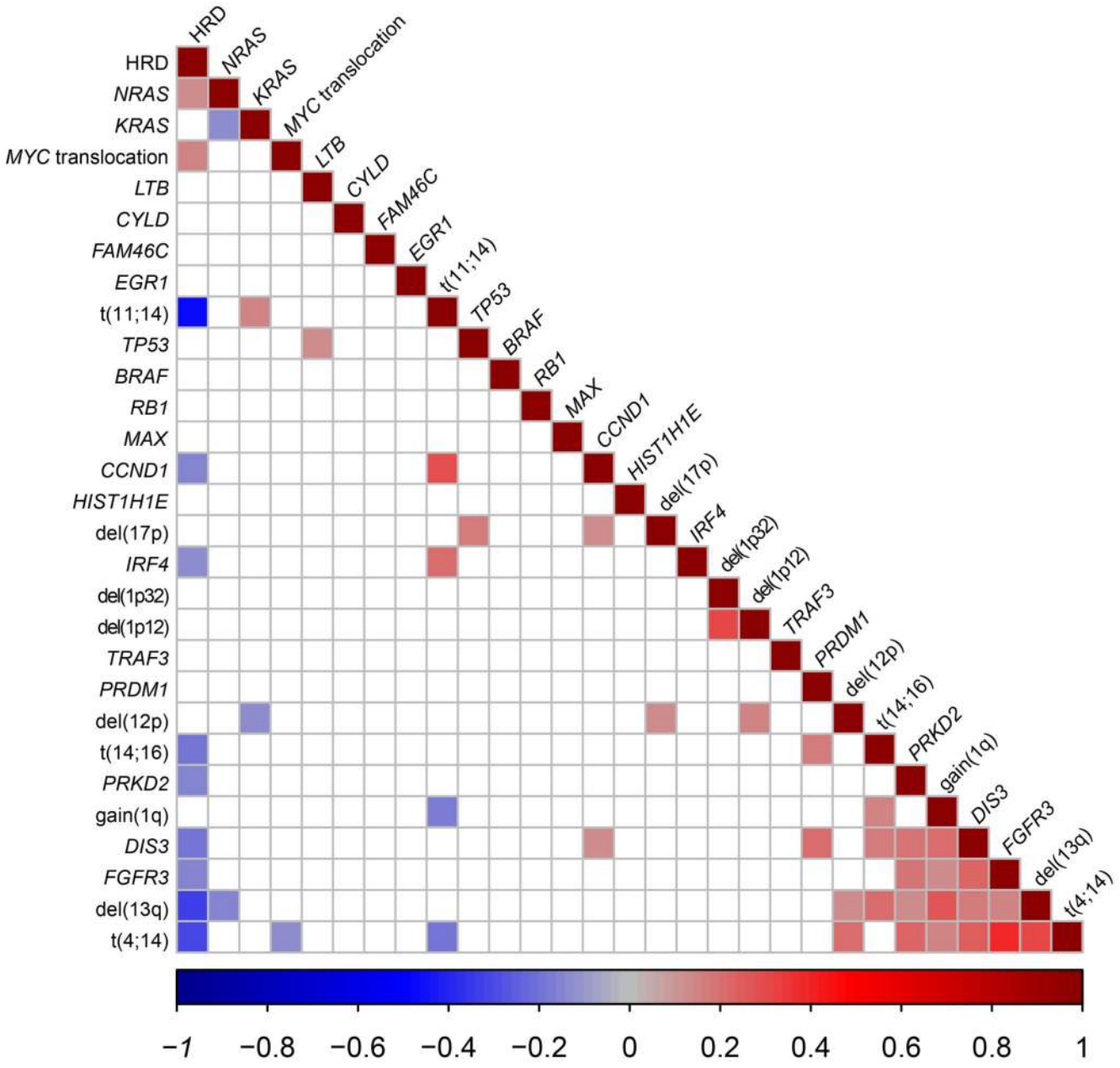

Figure 1.

Correlation between mutations and recurrent cytogenetic abnormalities. Intensity of colour shade represents the degree of correlation (blue=negative and red=positive) as per scale. Only significant correlations are represented on this plot with the insignificant correlations are in white.

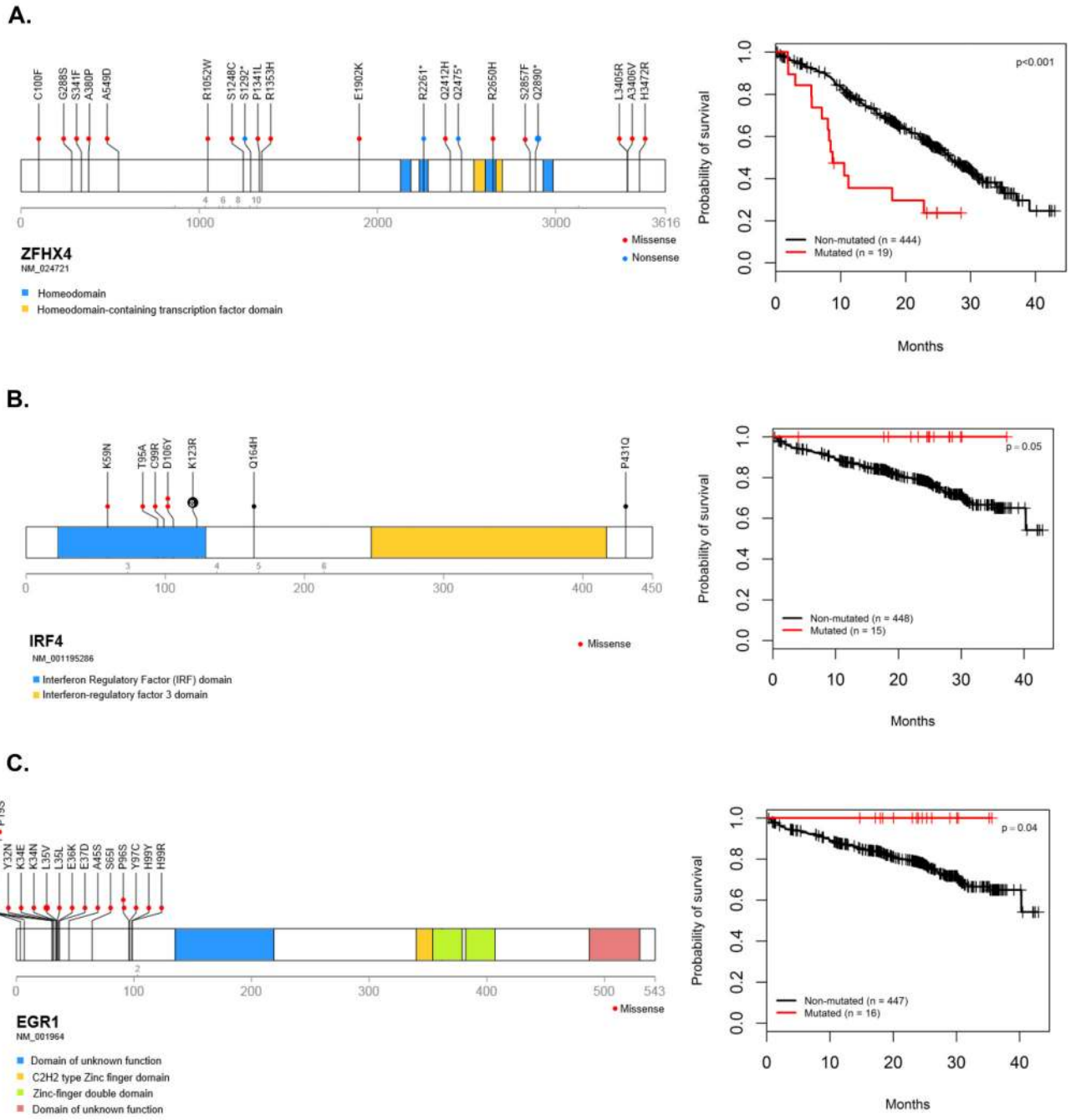

Figure 2.

Impact of DNA repair pathway alterations and CKS1B copy number changes in myeloma. The prognostic impact of the number of copies of amp(1q) is greater than gain(1q) for both PFS (A) and OS (B). *TP53* mutations and deletions are also associated with a significant negative impact on PFS (C) and OS (D). *ATM* and *ATR* mutations are associated with a worse outcome on both PFS (E) and OS (F).

Europe PMC Funders Author Manuscripts

Europe PMC Funders Author Manuscripts

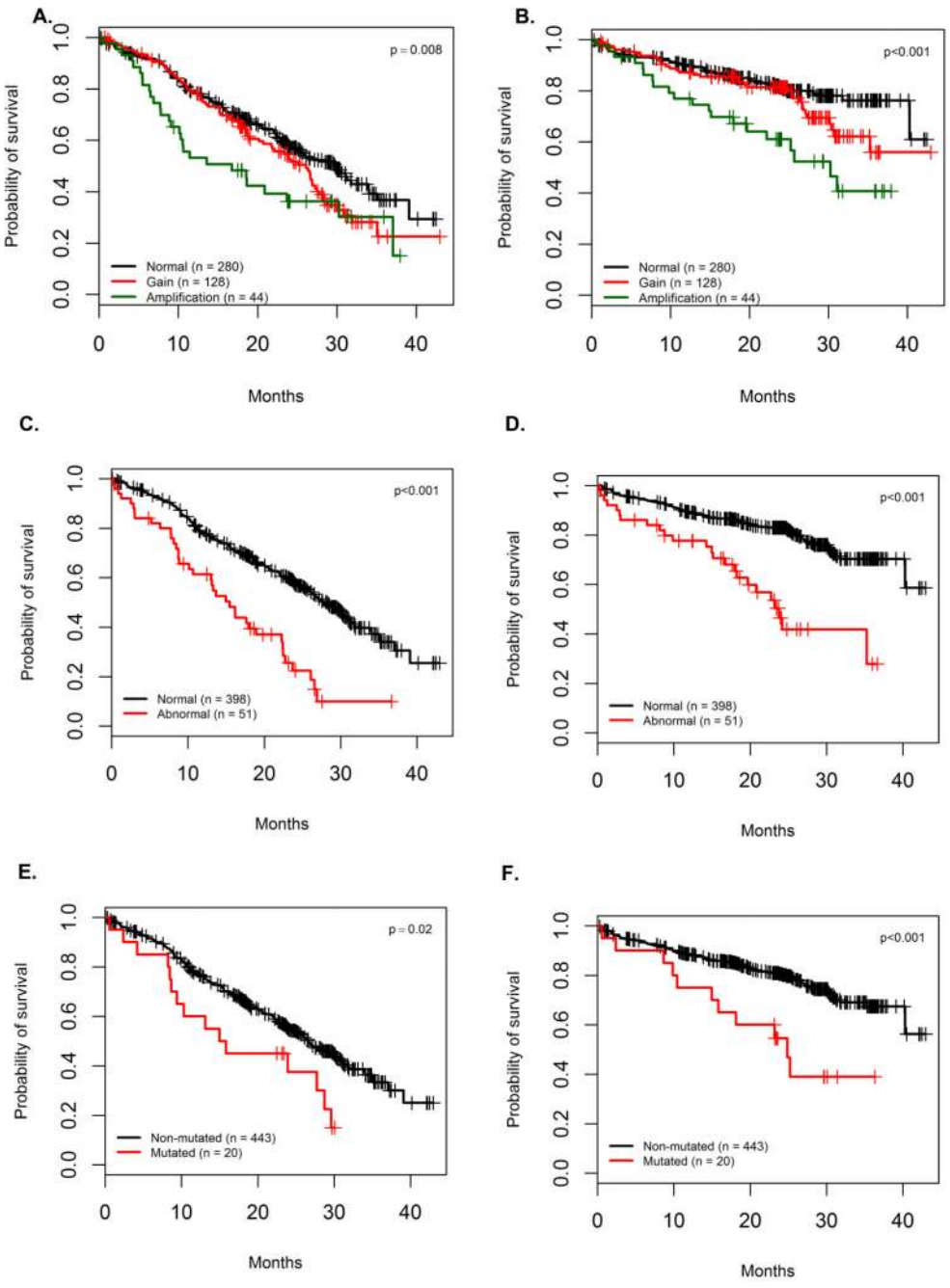

Figure 3.

Clinical impact and location of mutations in selected genes. Panel A: Location of the mutations and impact of *ZFHX4* mutations on PFS. Panel B: Location of the mutations and impact of *IRF4* mutations on OS. Panel C: Location of the mutations and impact of *EGR1* mutations on OS

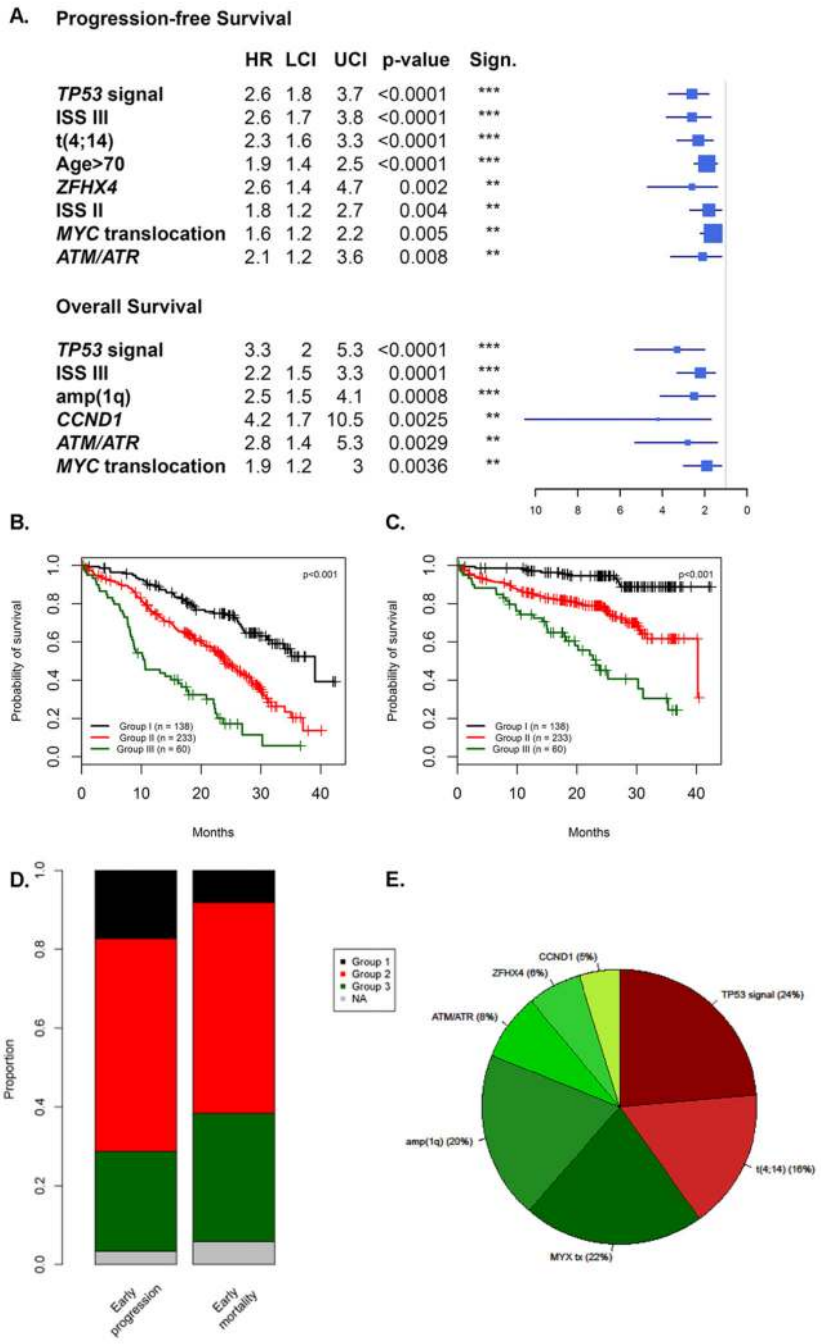

Figure 4.

Results of multivariate analysis (Panel A). The ISS-MUT identifies 3 prognostic groups (Group 1: ISS I/II with no CNSA or mutation, Group 2: ISS III with no CNSA or mutation or ISS I/II/III with one CNSA or mutation, Group 3: Two CNSA or mutation regardless of their ISS). It is an efficient tool to identify independent prognostic groups in terms of PFS (Panel B) and OS (Panel C). It also identified 81% and 90% of patients that both relapse and die prematurely (panel D) The adverse features that make up the HR group in the ISS-MUT score comprises not only the traditional ISS-FISH lesions, t(4;14) and del(17p) but also a

variety of lesions previously not considered in the score that account for approximately 60% of the lesions (panel E).

Europe PMC Funders Author Manuscripts

Table 1

Significantly mutated genes and their distributions in the main cytogenetic subgroups.

Gene	Group	Samples with mutation in group (%)	Non-synonymous Mutations (n=)	Synonymous Mutations (n=)	p-value	q-value
Overall						
HIST1H1E	All	2.8	15	1	$< 9\times10^{-18}$	$< 9\times10^{-18}$
IRF4	All	3.2	15	1	$< 9\times10^{-18}$	$< 9\times10^{-18}$
KRAS	All	21.1	104	0	$< 9\times10^{-18}$	$< 9\times10^{-18}$
MAX	All	2.4	13	0	$< 9\times10^{-18}$	$< 9\times10^{-18}$
NRAS	All	19.4	91	0	$< 9\times10^{-18}$	$< 9\times10^{-18}$
TP53	All	3.0	16	0	$< 9\times10^{-18}$	$< 9\times10^{-18}$
TRAF3	All	3.7	19	0	$< 9\times10^{-18}$	$< 9\times10^{-18}$
FAM46C	All	5.6	26	1	5.00×10^{-15}	1.05×10^{-11}
DIS3	All	8.6	48	1	5.88×10^{-15}	1.11×10^{-11}
BRAF	All	6.7	36	0	8.77×10^{-15}	1.50×10^{-11}
LTB	All	3.0	14	1	2.84×10^{-8}	4.46×10^{-5}
CYLD	All	2.4	14	0	6.65×10^{-6}	9.66×10^{-3}
RB1	All	1.5	7	0	1.96×10^{-5}	2.64×10^{-2}
t(4;14)						
DIS3	t(4;14)	25.4	18	0	7.05×10^{-8}	1.33×10^{-3}
FGFR3	t(4;14)	16.9	12	0	6.93×10^{-7}	6.54×10^{-3}
t(11;14)						
KRAS	t(11;14)	33.7	31	0	$< 9\times10^{-18}$	$< 9\times10^{-18}$
NRAS	t(11;14)	25.6	22	0	1.44×10^{-15}	1.36×10^{-11}
DIS3	t(11;14)	11.6	12	0	5.74×10^{-6}	3.61×10^{-2}
IRF4	t(11;14)	10.5	9	0	1.18×10^{-5}	5.57×10^{-2}
Hyperdiploidy						
KRAS	HRD	20.6	54	0	$< 9\times10^{-18}$	$< 9\times10^{-18}$
NRAS	HRD	24.4	53	0	$< 9\times10^{-18}$	$< 9\times10^{-18}$
FAM46C	HRD	7.1	15	1	6.99×10^{-9}	4.40×10^{-5}
BRAF	HRD	6.7	16	0	1.45×10^{-6}	6.85×10^{-3}
EGR1	HRD	4.6	11	1	4.65×10^{-6}	1.70×10^{-2}
CYLD	HRD	2.9	11	0	1.89×10^{-5}	5.09×10^{-2}

Table 2

Prognostic impact of the main variables in myeloma. Median survivals for mutations, CNSA and clinical variables are summarised in this table. NS stands for nonsignificant. NR for not reached.

	PFS present (months)	PFS absent (months)	p value	2 year-OS present (%)	2 year-OS absent (%)	p value	Frequency (%)
Clinical features							
Age>70	18.7	30.5	<0.0001	76%	81%	0.06	40%
Creatinine >150	18.7	27.7	0.0003	67%	81%	0.0009	12%
ISS I	39.1		-	87%		-	30%
ISS II	27.3		0.01	79%		0.13	29%
ISS III	22.0		<0.0001	74%		0.0004	34%
Mutations							
ZFHX4	8.8	26.9	<0.0001	72%	80%	NS	4%
TP53	13.7	26.9	0.0005	27%	81%	0.0001	3%
ATM/ATR mutations	15.4	26.6	0.02	55%	81%	0.0008	4%
IRF4	Not reached	26.1	0.09	100%	79%	0.05	3.2%
EGR1	35.1	26.1	NS	100%	79%	0.04	3.5%
CCND1	10.7	26.6	NS	38%	80%	0.005	2.2%
NCKAP5	10.6	26.6	NS	53%	80%	0.04	2.2%
Translocations and copy number abnormalities							
Del(17p)[*TP53*]	15	27.5	<0.0001	52%	82%	<0.0001	9.5%
t(4;14)	16.7	27.7	0.0001	71%	80%	0.08	12.7%
Del(13q)	22.7	28.7	0.0008	75%	82%	NS	42.1%
Normal 1q [*CKS1B*]	29.7		-	81%		-	61%
Gain(1q) [*CKS1B*]	26.1		NS	81%		NS	28%
Amp(1q) [*CKS1B*]	16.8		0.004	61%		0.0002	9.5%
Hyperdiploidy	29.6	23.7	0.009	81%	77%	NS	51.4%
***MYC* translocation**	21.7	27.5	0.008	68%	82%	0.006	18.4%
Del(12p)	22.7	26.7	0.015	68%	80%	0.09	8.9%
MAF translocations	17.6	26.6	NS	65%	80%	NS	4.5%
Del(1p)[*FAF1 CDKN2C*]	21.7	26.7	NS	58%	81%	0.001	8.4%
t(14;16)	17.6	26.6	NS	69%	80%	NS	3.8%
Del(1p) [*FAM46C*]	26.6	26	NS	79%	79%	NS	24%
Del(16q)	27	25.8	NS	77%	81%	NS	18.6%
t(11;14)	26.6	26.1	NS	78%	79%	NS	18.6%
Del(14q32) [*TRAF3*]	26.9	26.3	NS	80%	79%	NS	13.2%
Pathways							
***TP53* signal** *	15.4	28.4	<0.0001	46%	83%	<0.0001	11%
***DIS3* signal** *	22.1	28.5	0.001	77%	81%	NS	40.2%
***FAM46C* signal** *	26.9	25.5	NS	79%	79%	NS	27%

Europe PMC Funders Author Manuscripts

	PFS present (months)	PFS absent (months)	p value	2 year-OS present (%)	2 year-OS absent (%)	p value	Frequency (%)
***RAS* mutated**	27.5	23.9	NS	80%	78%	NS	43%
***FAF1* signal** *	22.8	26.7	NS	62%	81%	0.001	9.9%
NF-κB signal *	25.5	26.6	NS	78%	81%	NS	37%

* **Signal refers to the combination of mutations and copy number changes**

Europe PMC Funders Author Manuscripts

Table 3

Actionable mutations. Tumour fractions and percentage of mutations are presented in this table with an example of agent and the phase of development that may be used

Gene	Tumour fraction	n	% patients	Example	Phase (cancer)
KRAS	32.3%	98	21.17%	MEK inhibitor	Phase III
NRAS	33.6%	90	19.44%	MEK inhibitor	Phase III
BRAF	25.2%	31	6.70%	Vemurafenib	Phase III
CCND1	41.7%	10	2.16%	Pablociclib	Phase I
FGFR3	37.1%	10	2.16%	Masitinib	Phase II
MLL	29.1%	8	1.73%	EPZ-5676	Phase I
ROS1	41.3%	8	1.73%	Foretinib	Phase II
RET	33.4%	6	1.30%	Cabozantinib	Phase II
ERBB4	42.3%	5	1.08%	Lapatinib	Phase II
FLT3	44.0%	5	1.08%	Sunitinib	Phase III
ERBB2	11.9%	3	0.65%	Herceptin	Phase III
FGFR2	66.7%	3	0.65%	Masitinib	Phase II
KIT	40.9%	3	0.65%	Ponatinib	Phase III
MAP2K1	14.9%	3	0.65%	MEK inh	Phase III
ABL1	53.3%	2	0.43%	Gleevec	Phase III
BRCA2	52.2%	2	0.43%	PPARP inhibitor (BMN673)	Phase I
DNMT3A	39.2%	2	0.43%	5-azacytidin	Phase III
EGFR	21.7%	2	0.43%	Erlotinib	Phase III
EPHB2	37.8%	2	0.43%	Herceptin	Phase III
PDGFRA	17.4%	2	0.43%	pazopanib	Phase I
BRCA1	6.4%	1	0.22%	PPARP inhibitor (BMN673)	Phase I
DDR2	58.3%	1	0.22%	Dasatinib	Phase III
FGFR4	28.6%	1	0.22%	Masitinib	Phase II
HIF1A	13.5%	1	0.22%	PX-478	Phase I
IDH2	17.9%	1	0.22%	AG-221	Phase I
KIF5B	5.9%	1	0.22%	Cabozantinib	Phase II
MET	39.8%	1	0.22%	MSC2156119J	Phase I
MPL	51.9%	1	0.22%	Eltrombopag	Phase III
PIK3CA	45.1%	1	0.22%	GDC-0941	Phase I
RARA	10.2%	1	0.22%	ATRA	Phase III